

**CHAPTER V**  
**INFLUENCE OF IONIC STRENGTH ON COMPLEX FORMATION**  
**BETWEEN POLY(ETHYLENE OXIDE) AND CATIONIC SURFACTANT**  
**AND TURBULENT WALL SHEAR STRESS IN AQUEOUS SOLUTION**

**5.1 Abstract**

We investigate the influence of ionic strength on the interaction between poly(ethylene oxide) (PEO) and cationic surfactant, hexadecyltrimethylammonium chloride (HTAC), and the consequent effect on turbulent drag reduction by aqueous PEO/HTAC solutions. Conductivity and surface tension data for PEO-HTAC in aqueous solution indicate that salt stabilizes binding of HTAC micelles to the polymer. Dynamic light scattering analysis indicates an increase in hydrodynamic radius for HTAC micelles in aqueous salt solution. In contrast, salt reduces the hydrodynamic radius of PEO-HTAC complexes. The latter observation is consistent with contraction of the PEO-HTAC complex via electrostatic screening. Measurement of drag reduction efficiency using a double Couette rheometer indicates that minimum wall shear stress (maximum drag reduction) for aqueous HTAC occurs at an optimum HTAC concentration, whose value is comparable to the CMC and it decreases with increasing ionic strength. This surprising result suggests lowering of the CMC in turbulent flow. For aqueous PEO-HTAC mixtures, minimum wall shear stress occurs at an optimum PEO concentration, which is smaller than that of pure PEO, and whose value increases with ionic strength. Our results demonstrate a new concept that the turbulent wall shear stress does not always scale inversely with hydrodynamic volume of the complex.

**5.2 Introduction**

The addition of small amounts of high-molecular weight polymers or surfactants to a fluid in a fully developed turbulent flow can cause a dramatic reduction of the turbulent wall shear stress [1,2,3]. This phenomenon, known as

turbulent drag reduction (DR), was discovered more than fifty years ago [4]. Numerous applications of DR are known, including transportation of crude oil in oil pipelines, increased jet velocity and beam focusing in fire fighting equipment, prevention of over dosage of water flow during heavy rain in drainage and irrigation systems, increase of volumetric flow rate of fluid in hydro-power systems and improvement of blood flow in partially blocked arteries in biomedical studies [5,6,7,8,9].

The mechanism of turbulent drag reduction has been explored extensively since the original discovery by Toms [4], who, prompted by Oldroyd's theory of wall slip [10], first proposed the idea that the polymer creates a shear thinning layer at the wall having an extremely low viscosity. Subsequently, Lumley [11-13] suggested that there is a critical value of wall shear stress, at which macromolecules become stretched due to the fluctuating strain rate. However, in the laminar sublayer close to the wall, polymer coils are not greatly deformed and viscosity does not increase greatly above that of the solvent alone. In the turbulent zone, the macromolecular extension yields a dramatic increase in viscosity, which damps small dissipative eddies, and reduces momentum transport towards the laminar sublayer, resulting in a thickening of the sublayer and a reduction of the drag. Virk [14] suggested that, at the onset of turbulent drag reduction, the duration of a turbulent burst is of the order of the terminal relaxation time of a macromolecule, and proposed that energy dissipation via macromolecular extension is involved in the mechanism of drag reduction. Hlavacek et al. [15] proposed that, in turbulent flow, the solvent contains microdisturbances or turbulence precursors. Macromolecules suppress turbulence by pervading two or more of these microdomains simultaneously and hindering their free movement and growth. De Gennes [16,17] developed a model based on the Kolmogorov energy cascade theory, and considering the ability of polymer molecules to store elastic energy upon deformation. When this elastic energy is comparable to the kinetic energy of a particular turbulent eddy, the energy cascade is suppressed. Ryskin [18] proposed the yo-yo model, as the mechanism by which polymer molecules unravel in an extensional flow field associated with turbulence. The central portion of the chain straightens, while the end portions remain coiled. When the flow becomes weak, the polymer chain retracts into a fully-coiled state.

The taut central portion generates a large stress and facilitates viscous dissipation of turbulent kinetic energy.

Polymers and surfactants have received considerable attention among available drag reducing additives [19,20]. In general, effective drag reducing polymers should possess a linear flexible structure and a very high molecular weight [19]. One polymer known to be suitable for use as a drag reducer is poly(ethylene oxide) (PEO) [21]. This polymer is commercially available over a wide range of molecular weights. Previous studies [19, 22] report that drag reduction for PEO solutions is observed above a critical molecular weight,  $M_c$  (for the double Couette geometry used in our experiments [22],  $0.91 \times 10^5 < M_c < 3.04 \times 10^5$  g/mol). Maximum drag reduction occurs at an optimum concentration,  $c_{PEO}^*$ , which scales inversely with molecular weight, and the % maximum drag reduction increases with molecular weight [19,22]. However, polymers are susceptible to high shear degradation, and are therefore limited to a single throughput application. Certain surfactants form large wormlike or network microstructures in solution which are thermodynamically stable and self-assemble quickly after degradation, restoring drag reducing power. For this reason, they have become of increasing interest as drag reducing additives in the last decade. Among the drag reducing surfactants, the cationic species (hexadecyltrimethyl ammonium chloride, HTAC) has been shown to be an effective drag reducer [23,24], when used in combination with organic counterions, which facilitate the formation of wormlike micellar structures.

Recent studies have demonstrated that water-soluble polymers like PEO form complexes with cationic surfactants such as HTAC [25-28] in which surfactant micelles are bound to the polymer. The formation of such complexes causes characteristic changes in solution viscosity, because of the increased hydrodynamic volume of the complex. In a previous study [22], we investigated the effect of complex formation between PEO and HTAC on the drag reduction behavior of PEO solutions, and showed that the critical PEO molecular weight for drag reduction decreases, interpreted as due to the increase in hydrodynamic volume when HTAC micelles bind to PEO. Also, consistent with this interpretation, at fixed PEO concentration, maximum drag reduction is observed at an optimum HTAC concentration,  $c_{HTAC-PEO}^*$ , comparable to the maximum binding concentration, MBC,

where polymer chains are saturated with surfactants [22]. Moreover, with HTAC concentration fixed at the MBC, the optimum PEO concentration for drag reduction,  $c^*_{\text{PEO-HTAC}}$ , decreases relative to that,  $c^*_{\text{PEO}}$ , in the absence of HTAC [22].

Addition of salt stabilizes the binding of HTAC micelles to the PEO due to the screening of electrostatic repulsions between the surfactant headgroups [28]. The number of PEO chains incorporated into PEO-HTAC complexes in aqueous salt solution is smaller than that in the salt-free PEO-HTAC complex [28], i.e. dissociation of multichain complexes occurs in the polymer-surfactant complex solutions when salt is added [28]. These observations motivate the present study, first, to investigate the effect of ionic strength on the hydrodynamic radius of pure surfactant in solution and compare the results with those for the polymer-surfactant complex. Second, we study the consequent effect of these changes in structure on turbulent drag reduction. Based on these observations, we discuss whether polymer-surfactant complex formation survives under turbulent flow conditions, and hence produces a synergistic response in the drag reduction characteristics of PEO and HTAC in aqueous salt solution.

### 5.3 Experimental Section

Poly (ethylene oxide) (PEO) of quoted molecular weights  $6.00 \times 10^5$  and  $40.0 \times 10^5$  g/mol, designated PEO6 and PEO20 were purchased from Aldrich Chemical Co. and used without further purification. The cationic surfactant was Hexadecyltrimethylammonium Chloride, (HTAC,  $\text{C}_{16}\text{H}_{33}\text{N}(\text{CH}_3)_3\text{Cl}$ ), a commercial product donated by Unilever Holding Inc., used as received. The surfactant solution contains 50 % HTAC, 36 %  $\text{H}_2\text{O}$  and 14 % isopropanol. Analytical grade sodium chloride (NaCl), at 99.5 % minimum assay (Carlo Erba Reagenti Co.) was used to vary ionic strength of the complex solutions. Distilled water was used as a solvent after two times filtration through  $0.22 \mu\text{m}$  Millipore membrane filters to remove dust particles. The polymer stock solutions were prepared as % w/v in distilled water at room temperature by dissolving PEO in distilled water and by gentle stirring for a period of 4 – 10 days, depending on polymer concentration and molecular weights. Surfactant and polymer-surfactant complex solutions were prepared by adding

appropriate amounts of HTAC and NaCl into mixtures of distilled water and polymer stock solutions and by gentle stirring for 24 h at room temperature. Before light scattering measurements, the polymer-surfactant complex solutions were centrifuged at 10,000 rpm for 15 min and then filtered directly into the light-scattering cell through 0.45  $\mu\text{m}$  Millipore membranes. All measurements were carried out at a temperature of 30°C.

#### 5.4 Results and Discussions

The physicochemical properties of aqueous solutions of surfactant-polymer complexes were investigated at 30°C. As noted in Table 5.1, two specimens were utilized, PEO6 and PEO20, whose weight-average molecular weights,  $M_w$ , were determined from SLS measurement to be  $6.06 \times 10^5$  g/mole and  $17.9 \times 10^6$  g/mole, respectively. The measured  $M_w$  for PEO6 is quite close to the manufacturer quoted value, whereas, for PEO20, the measured  $M_w$  is substantially smaller. This suggests that the high-end portion of the molecular weight distribution was removed during filtration of solutions prior to experimental measurements. Previous studies [22] showed that the optimum PEO concentrations,  $c_{\text{PEO}}^*$ , for maximum drag reduction in pure PEO solutions, measured as the minimum value of  $\tau_w$  in the double Couette rheometer via eq. (7) are 40 ppm (0.91 mM/PEO repeating unit) and 15 ppm (0.34 mM/PEO repeating unit) for specimens PEO6 and PEO20, respectively. Table 1 lists values of the critical aggregate concentration, CAC, corresponding to the onset of surfactant binding to the polymer, the critical micelle concentration, CMC, at which free micelles form in the surfactant-polymer solution, and the maximum binding concentration, MBC, the surfactant concentration at which the PEO becomes saturated with bound surfactant. The CAC, CMC, and MBC were determined, as described below, from measurements of conductivity and surface tension of PEO-HTAC complexes in aqueous NaCl solutions, whose PEO concentrations were fixed at the respective values,  $c_{\text{PEO}}^*$ , where the maximum drag reduction of PEO solutions is observed in the absence of surfactant.

#### 5.4.1 Critical Aggregate Concentration, CAC, Critical Micelle Concentration, CMC, and Maximum Binding Concentration, MBC

The CAC, CMC were determined at 30°C by two methods: conductivity and surface tension; the MBC was determined from surface tension measurements. Figures 5.1-5.3 show conductivity as a function of HTAC concentration for aqueous solutions of HTAC and HTAC-NaCl (Figure 5.1), PEO6-HTAC, and PEO6-HTAC-NaCl mixtures (Figure 5.2), and PEO20-HTAC, and PEO20-HTAC-NaCl mixtures (Figure 5.3). The PEO6 concentration was fixed at  $c_{\text{PEO}}^* = 40$  ppm while the PEO20 concentration was set at  $c_{\text{PEO}}^* = 15$  ppm, and, in each case, two different values of mole ratio were investigated,  $[\text{NaCl}]/[\text{HTAC}] = 1/1$  and  $5/1$ . In Figures 5.1a-5.1c, the first and only transition in slope of a plot of conductivity versus HTAC concentration identifies the CMC for HTAC and HTAC-NaCl solutions. In Figures 5.2 and 5.3, the CAC is identified as the initial change in slope, and the CMC as the second slope change. However, the CAC is clearly discernable only in the absence of salt (Figures 5.2a and 5.3a), and therefore surface tension measurements had to be used instead. The corresponding CAC and CMC values are listed in Table 5.1.

Figure 5.4 exhibits the variation of surface tension with HTAC concentration for PEO6-HTAC solutions having PEO6 at 40 ppm, without salt, and with salt added at mole ratios  $[\text{NaCl}]/[\text{HTAC}]$  of 1.0 and 5.0. As evident in Figure 5.4, the surface tension decreases on addition of HTAC, and the CAC values is located as the initial HTAC concentration at which a discrete change to a regime of constant surface tension occurs. Subsequently, the surface tension begins to decrease again, and this point is identified as the MBC, i.e. where the PEO chains have become saturated with bound HTAC. Finally a third transition point occurs where the surface tension levels off and no further decrease occurs with addition of HTAC. This corresponds to the CMC. These characteristic transitions are indicated by arrows in Figure 5.4, and the corresponding CAC, MBC, and CMC values are listed in Table 5.1.

From Table 5.1, we see that the CAC and CMC values for PEO-HTAC complexes in aqueous solution from surface tension are consistent with those obtained from conductivity. We also find that the CAC and CMC values in salt



solution are lower than in water. Increase in ionic strength, promotes the formation of HTAC micelles and PEO-HTAC complexes due to a reduction in electrostatic repulsions between the ionic surfactant head groups which stabilizes the surfactant micelle structure, as shown previously [28]. We further find that, at a given NaCl/HTAC mole ratio, the CMC values of the PEO-HTAC solutions are higher than those of the pure surfactant. The increase of the CMC in PEO-HTAC complex solutions corresponds quantitatively to the amount of PEO-bound surfactant. Finally, from Table 5.1, we find that, as salt is added a higher MBC value is observed, which, combined with a decreasing trend in CAC, indicates an increase in the amount of surfactant molecules bound to the PEO chains, again reflective of an increase in PEO-HTAC complex stability due to the screening of electrostatic repulsions between surfactant head-groups. Table 5.1 also contains results for solutions containing high molecular weight PEO, i.e. PEO20 at 15 ppm without salt, and with added salt, having mole ratios  $[\text{NaCl}]/[\text{HTAC}] = 1/1$  and  $5/1$ . Uncertainties of the data obtained from surface tension measurement typically vary within 10%. However, it appears that there is no substantive change in surface tension values when comparing the solutions containing HTAC complexed to high versus low molecular weight (PEO20 at 15 ppm c.f. PEO6 at 40 ppm). This result is consistent with the previous observation of Schwuger [31] who found that the surface tension of solutions of PEO, complexed with an anionic surfactant, SDS, (PEO  $M_w > 4000$ ) was independent of PEO molecular weight. The MBC values of PEO-HTAC solutions are tabulated in Table 5.1.

To summarize the above results, the addition of salt leads to a reduction of the CMC and CAC but an increase in MBC of PEO-HTAC solutions. These effects indicate, respectively, a reduction in electrostatic repulsions between the positive surfactant head groups of micelles and an increase in binding affinity between the surfactant and the PEO chain.

#### 5.4.2 Dynamic Light Scattering Measurements

Table 5.2 lists values of the diffusion coefficient,  $D_o$ , hydrodynamic radius,  $R_h$ , and normalized second cumulant,  $\mu_2 / \bar{\Gamma}^2$  obtained from dynamic light scattering

measurement of aqueous PEO-HTAC-NaCl complex solutions at 30°C. Uncertainties indicate standard deviations obtained from repeated measurements on the same samples. For HTAC and NaCl-HTAC solutions,  $D_o$ ,  $R_h$  and  $\mu_2 / \bar{\Gamma}^2$ , were determined at the corresponding CMC. The micellar radii,  $R_h$ , in the absence of salt and with salt added at molar ratios  $[\text{NaCl}]/[\text{HTAC}] = 1/1$  and  $5/1$  are, respectively, 1.31, 2.23, and 2.47 nm, indicating that, as expected, added salt increases the aggregation number and size of HTAC micelles. For PEO6 and PEO20 solutions,  $D_o$ ,  $R_h$ , and  $\mu_2 / \bar{\Gamma}^2$  were determined at 5.0 mM HTAC, the maximum HTAC concentration investigated in wall shear stress measurements. However, for PEO20, we also measured  $D_o$ ,  $R_h$ , and  $\mu_2 / \bar{\Gamma}^2$  at HTAC concentrations equal to 0.2 mM i.e. near the MBC. In all cases, Table 2 shows that the hydrodynamic radius of PEO-HTAC complexes is observed to be largest in the absence of added salt. The addition of salt at a mole ratio of  $[\text{NaCl}]/[\text{HTAC}] = 1/1$  decreases  $R_h$ , substantially, but a further increase of salt to a mole ratio of  $\text{NaCl}/\text{HTAC} = 5/1$  results in a slight increase in  $R_h$ . Our results are consistent with the previous published data reported by Khine et al.[28], who compared  $R_h$  values at MBC for PEO-HTAC solutions in the absence of added salt and with 0.1 M  $\text{KNO}_3$  added. Addition of 0.1 M  $\text{KNO}_3$  was observed to reduce the value of  $R_h$ , due to the combined effects of polymer chain contraction via electrostatic screening and dissociation of multichain complexes. The reason for the small increase in  $R_h$  at higher salt is not clear, but may reflect an increase in the bound micellar radius, analogous to that observed in free micelles.

Finally, we comment on results for the normalized second cumulant,  $\mu_2 / \bar{\Gamma}^2$  which is a measure of the variance in the distribution of hydrodynamic radii. For HTAC and HTAC-NaCl with a mole ratio of 5,  $\mu_2 / \bar{\Gamma}^2$  values are 0.16 and 0.07, respectively. For PEO6\_40+HTAC 5 mM and PEO6\_40+HTAC 5 mM+[NaCl]/[HTAC]=5/1,  $\mu_2 / \bar{\Gamma}^2$  values are 0.83 and 0.23, respectively. For PEO20\_15+HTAC 0.2 mM and PEO20\_15+HTAC 0.2 mM+[NaCl]/[HTAC]=5/1,  $\mu_2 / \bar{\Gamma}^2$  values are 0.45 and 0.34, respectively. These



results indicate that addition of salt reduces the size polydispersity of micelle and complex structures formed.

### 5.4.3 Wall Shear Stress Measurements

Figure 5.5 exhibits the variation of wall shear stress,  $\tau_w$ , at  $Re = 5000$ , as HTAC concentration is increased for HTAC solutions at  $30^\circ C$ , without salt, and with salt added at mole ratios  $[NaCl]/[HTAC]$  equal to 1.0 and 5.0. For salt-free HTAC, the wall shear stress decreases with increasing concentration up to an optimum concentration,  $c_{HTAC}^* = 1.7$  mM, where we find a maximum drag reduction of about 51 %. Above  $c_{HTAC}^*$ , the wall shear stress shows a slight increase with HTAC concentration. With salt added at NaCl/HTAC mole ratios of 1.0 and 5.0, the wall shear stresses of these solutions initially decreases as the salt-free solution, but exhibits minima at optimum concentrations,  $c_{HTAC}^* \approx 0.9$  and 0.3 mM, respectively, which are much smaller than the salt-free case, after which a sharp rise to a constant value is seen. The corresponding maximum drag reductions are 56% and 39%, respectively. Here, we note that the CMC of HTAC in aqueous HTAC,  $[NaCl]/[HTAC] = 1/1$  and  $[NaCl]/[HTAC] = 5/1$  solutions occurs at approximately 1.3, 0.7 and 0.6 mM; respectively. These values are numerically comparable to the respective optimum HTAC concentrations of those solutions, so we observe significant an apparent drag reduction prior to micelle formation. This is an unexpected result, and its origin is presently unclear. Any contribution to the wall stress from lowering of the surface tension is expected to be negligible. The only possibility which seems to present itself is that the CMC is somehow reduced in the turbulent flow field. Recent work [32] suggests that the mixed shear and extensional character of such flows may promote micelle formation leading to local concentrations of surfactant that are much larger than the mean value. In micelle-driven drag reduction, the optimum HTAC concentration decreases with ionic strength, because the micellar size increases with ionic strength, due to neutralization of electrostatic repulsions between surfactant headgroups [33,34,35]. We further observe in Figure 5.5 an increase in wall shear stress or a diminished drag reduction

in the presence of added salt at HTAC concentrations beyond the CMC. We attribute this to the increased viscous resistance because of the presence of increasing numbers of micelles.

Figure 5.6 shows the dependence of wall shear stress,  $\tau_w$ , on HTAC concentration at  $Re = 5000$  and at  $30^\circ\text{C}$  for PEO6\_40+HTAC, PEO6\_40+[NaCl]/[HTAC] = 1/1 and PEO6\_40+[NaCl]/[HTAC] = 5/1, respectively. Here, we find that wall shear stress of PEO6\_40+HTAC monotonically increases with increasing HTAC concentration, to an essentially constant value as the HTAC concentration approaches the CMC ( $CMC_{\text{PEO6}_40+\text{HTAC}} = 1.70 \text{ mM}$ ). Likewise, the wall shear stresses of PEO6\_40+[NaCl]/[HTAC] = 1/1 and PEO6\_40+[NaCl]/[HTAC] = 5/1 increase with HTAC concentration to a maximum value near their respective CMCs ( $CMC_{\text{PEO6}_40+[\text{NaCl}]/[\text{HTAC}] = 1/1} = 1.50 \text{ mM}$  and  $CMC_{\text{PEO6}_40+[\text{NaCl}]/[\text{HTAC}] = 5/1} = 1.00 \text{ mM}$ ), after which, the wall shear stresses decrease to smaller asymptotic values at HTAC concentrations in excess of 4.0 mM. Recalling that the PEO concentration is fixed at the optimum concentration for drag reduction in the absence of surfactant ( $c^*_{\text{PEO}}$ ), the observed increase in wall stress on titration with HTAC was demonstrated in our earlier work [22] to arise because the presence of HTAC causes a shift in  $c^*_{\text{PEO}}$  from 40 mM to lower PEO concentration. Figure 6 further shows that the increase in the wall stress occurs at very low added levels of HTAC, below the nominal CAC and MBC values (Table 1). As noted and confirmed in our earlier study [22], this implies that the CAC and MBC are presumably reduced in turbulent flow, which allows a shift of the optimum HTAC concentration,  $c^*_{\text{HTAC-PEO}}$  to a lower value. A third feature of Figure 5.6 is that, when the HTAC concentration is above the MBC, increase in the NaCl/HTAC mole ratio produces a decrease in wall shear stress. This effect may be attributed to a decrease in the hydrodynamic volume, confirmed by DLS measurements (Table 5.2) because the increased ionic strength causes electrostatic screening between bound micelles, and therefore, chain contraction occurs. Alternatively, the decrease in the wall shear stress upon addition of salt to PEO-HTAC complex maybe related to the more stabilized PEO-HTAC complex formation and possibly to the reduction in the PEO chain rigidity resulting from the dissociation of multichain complexes. Our result is thus opposite to the generally accepted idea that turbulent wall shear stress decreases

with increasing hydrodynamic volume.

In Figure 5.7, we exhibit the variation in wall stress,  $\tau_w$ , with HTAC concentration at  $Re = 5000$  and  $30^\circ C$ , for PEO-HTAC solutions containing high molecular weight PEO, viz. PEO20\_15+HTAC, PEO20\_15+[NaCl]/[HTAC] = 1/1 and PEO20\_15+[NaCl]/[HTAC] = 5/1. The data displayed in Figure 7 show essentially the identical behavior to that seen in Figure 6 for lower molecular weight PEO. At high concentrations of HTAC, beyond the CMC,  $\tau_w$  is lowered in the presence of NaCl. An additional feature manifested in Figure 7 is that the initial rate of increase of  $\tau_w$  on titration with HTAC is clearly slower in the presence of added salt. This suggests that the presence of salt results in a smaller shift of the optimum concentration for drag reduction.

To confirm this, as shown in Figure 5.8, the dependence of wall shear stress on PEO concentration was examined at  $Re = 5000$  and  $30^\circ C$  for 15 ppm PEO20 in aqueous solution containing 0.20 mM HTAC (corresponding to the MBC of 15 ppm PEO20), without salt and with salt added at mole ratios [NaCl]/[HTAC] = 1/1 and 5/1. Figure 5.8 indicates that, indeed, the optimum PEO concentration for maximum drag reduction increases with addition of salt, having values  $c_{PEO/HTAC}^* = 5, 7$  and  $10$  ppm, at which the maximum DR values are 90%, 72% and 62%, for solutions with [NaCl]/[HTAC] = 0, 1 and 5, respectively. At low PEO concentration,  $c_{PEO} < 30$  ppm, the increase in the optimum PEO concentration and the increase in the wall shear stress with salt addition correlate approximately with the decreased hydrodynamic volume of the PEO-HTAC complexes due to the effects of polymer chain contraction via the electrostatic screening and the dissociation of multichain complexes (Table 5.2). At high PEO concentration,  $c_{PEO} > 30$  ppm, the wall shear stresses of PEO-HTAC complex in salt solution are higher than that in water, with the wall shear stress of the solution having [NaCl]/[HTAC] = 1 being slightly greater than that of [NaCl]/[HTAC] = 5. The wall stress in this region may have derived from the increased solution viscosity when salt is added. Noting that in this case, as PEO concentration increases, the surfactant content falls increasingly below the MBC level, perhaps the hydrodynamic volume of PEO is increased in the presence of salt for surfactant depleted complexes.

Figures 5.9a-5.9b illustrates schematic drawings of complexes formed in PEO + HTAC in the absence and in the presence of NaSal in aqueous solution, respectively, when HTAC concentration is above CMC. In the salt free aqueous solution, binding of micelles on multichain polymer-surfactant complexes occurs in the solution, and electrostatic repulsions lead to an increase in hydrodynamic volume of polymer-surfactant complex [27]. In the presence of salt, the number of bound HTAC molecules per chain increases substantially, i.e. the added salt stabilizes the binding of HTAC micelles to the polymer and single chain complexes are predominantly formed [28]. In addition, the hydrodynamic volume of PEO-HTAC complex in the presence of salt is reduced due to effects of polymer chain contraction via the electrostatic screening and the dissociation of multichain complexes.

## 5.5 Conclusions

We investigated the influence of ionic strength on CAC, CMC, MBC and hydrodynamic radius in aqueous solutions of HTAC and PEO-HTAC mixtures at 30°C. Consistent with literature results, the values of CAC and CMC from conductivity and surface tension measurements indicate that salt stabilizes micelle formation in HTAC solutions and, in PEO-HTAC solutions, enhances the binding of HTAC micelles to the polymer. We also observe an increase in hydrodynamic radius of HTAC micelles at the MBC of HTAC in the presence of added salt and a decrease in  $R_h$  for the PEO-HTAC complexes in salt solution. These observations can be described, on the one hand to screening of electrostatic repulsions between surfactant head groups on HTAC micelles, and on the other, to PEO chain contraction via electrostatic screening and dissociation of multichain PEO-HTAC complexes. Wall shear stress measurements on HTAC solutions reveals that the optimal concentration for maximum drag reduction decreases with increasing molar ratios of NaCl to HTAC. The possible mechanisms of drag reduction in these solutions may be a surface tension effect, the decrease in the number of free micelles in aqueous HTAC solution, the decrease in the CMC in the turbulent flow field, or several effects combined. In PEO solutions on titration with HTAC, the wall stress increases up to the CMC and then decreases or levels off. This is due to a shift of the optimum

concentration for drag reduction to a smaller value, the magnitude of the shift decreasing with increase of ionic strength.

## 5.6 Acknowledgements

S. Suksamranchit would like to acknowledge the financial support from the Thailand Research Fund (TRF), the RGJ grant no. PHD/0149/2543. This work was financially supported by the fund from MTEC, grant no. MT-43-POL-09-144-G, and the funds from the ADB Consortium Grant and the Conductive and Electroactive Polymer Research Unit of Chulalongkorn University. AMJ acknowledges financial support through NSF award DMR 0080114.

## 5.7 References

1. P.S. Virk and H. Baher, *Chemical Engineering Science*, 25 (1970) 1183.
2. G. D. Rose and K. L. Foster, *J. Non-Newtonian Fluid. Mech.*, 31 (1989) 59.
3. N.S. Berman, *Ann. Rev. Fluid Mech.*, 10 (1978) 47.
4. B.A. Toms, Some observations on the flow of linear polymer solutions through straight tubes at large Reynolds numbers, *Proc. 1st International Congress of Rheology*, vol. 2, North-Holland, Amsterdam, 1949, Section II, p.135.
5. J. Golda, *Chem. Eng. Commun.*, 43 (1986) 53.
6. R.P. Singh, in N.P. Chermisinoff (Ed.), *Encyclopedia of Fluid Mechanics*, Vol. 9, Gulf Publishing, Houston, 1990, Chapter 14.
7. R.A. Mostardi, L.C. Thomas, H.L. Green, F. VanEssen, R.F. Nokes, *Biorheology*, 15 (1978) 1.
8. A. G. Fabula, *Trans. ASME J. Basic Eng.*, 93D (1971) 453.
9. H.L. Greene, R.F. Mostardi and R.F. Wokes, *Polym. Eng. Sci.*, 20 (1980) 499.
10. J.G. Oldroyd, *Proc. 1st International Congress on Rheology*, Vol II, North Holland, Amsterdam, 1948, p. 180.
11. J.L. Lumley, *Ann. Rev. Fluid Mech.*, 1 (1969) 367.
12. J.L. Lumley, *J Polym. Sci., Macromolec. Rev.*, 7 (1973) 263.

13. J.L. Lumley, *Phys. Fluids.*, 20 (10) (1997) Pt II S64-S71.
14. P.S. Virk, *AIChE J.*, 21 (1975) 625.
15. B. Hlavacek, L.A. Rollin and H.P. Schreiber, *Polymer*, 17 (1976) 81.
16. P.G. De Gennes, *Physica*, 140A (1986) 9.
17. P.G. De Gennes, in A. Luigi (Ed.), *Introduction to polymer dynamics: An elastic theory of drag reduction*, Cambridge University Press, Cambridge, Great Britain, 1990, Chapter 4.
18. G. Ryskin, *Phys. Rev. Lett.* 59 (18) (1987) 2059.
19. H.J. Choi and M.S. Jhon, *Ind. Eng. Chem. Res.*, 35 (1996) 2993.
20. J. L. Zakin, B. Lu, H. W. Bewersdorff, *Rev. Chem. Eng.*, 14 (1998) 253.
21. R.W. Paterson and F.H. Abernathy, *J. Fluid Mech.*, 43 (1970) 689.
22. S. Suksamranchit, A. Sirivat and A.M. Jamieson, *J. Colloid and Interface Science*, 294 (2006) 212
23. J. Myska, Z. Lin and P. Stepanek, J.L. Zakin, *J. Non-Newtonian Fluid Mech.*, 97 (2001) 251.
24. J. Myska, Z. Chara, *Exp. Fluids*, 30 (2) (2001) 229.
25. O. Anthony and R. Zana, *Langmuir*, 10, (1994) 4048.
26. K.Y. Mya, A. Sirivat and A.M. Jamieson, *Langmuir*, 16 (2000) 6131.
27. K.Y. Mya, A. Sirivat and A.M. Jamieson, *Macromolecules*, 34 (2001) 5260.
28. K.Y. Mya, A. Sirivat and A.M. Jamieson, *J. Phys. Chem B*, 107 (2003) 5460.
29. W. Brown, J. Fundin and M.D. Miguel, *Macromolecules*, 26 (26) (1992) 7192.
30. B.H. Zimm, Dynamic of polymer molecules in dilute solution: viscoelasticity, flow birefringence and dielectric loss, *J Chem. Phys.*, 24 (1956) 269.
31. M.J. Schwuger, *J Colloid Interface Sci.*, 43 (1973) 491.
32. K. Arora, R. Sureshkumar, M.P. Scheiner and J.L. Piper, *Rheol. Acta*, 41 (2002) 25.
33. W. Brown, J. Fundin and M.D. Miguel, *Macromolecules*, 26 (26) (1992) 7192.
34. J. Myska, P. Stepanek and J.L. Zakin, *Colloid Polym Sci.*, 275 (1997) 254.
35. B. Lu, Y. Zheng, H.T. Davis, L.E. Scriven, Y. Talmon, and L. Zakin, *Rheol. Acta*, 37 (1998) 528.



**Table 5.1** Conductivity and surface tension data of PEO-HTAC-NaCl complexes in quiescent aqueous solution at 30°C

| Codes of system studied      | PEO<br>$M_w$<br>(g/mol) | $^a c_{PEO}^*$<br>(ppm) | Conductivity     |                  | $^c$ Surface Tension |             |                  |
|------------------------------|-------------------------|-------------------------|------------------|------------------|----------------------|-------------|------------------|
|                              |                         |                         | $^b$ CAC<br>(mM) | $^c$ CMC<br>(mM) | CAC<br>(mM)          | CMC<br>(mM) | $^d$ MBC<br>(mM) |
| HTAC                         | -                       | -                       | -                | 1.30             | -                    | 1.30        | -                |
| [NaCl]/[HTAC] = 1/1          | -                       | -                       | -                | 0.70             | -                    | N/A         | -                |
| [NaCl]/[HTAC] = 5/1          | -                       | -                       | -                | 0.60             | -                    | N/A         | -                |
| PEO6_40+HTAC                 | $6.06 \times 10^5$      | 40                      | 0.19             | 1.65             | 0.16                 | 1.70        | 0.25             |
| PEO6_40+[NaCl]/[HTAC] = 1/1  | $6.06 \times 10^5$      | 40                      | N/A              | 1.20             | 0.13                 | 1.20        | 0.27             |
| PEO6_40+[NaCl]/[HTAC] = 5/1  | $6.06 \times 10^5$      | 40                      | N/A              | 1.00             | 0.13                 | 1.15        | 0.35             |
| PEO20_15+HTAC                | $17.9 \times 10^5$      | 15                      | 0.19             | 1.80             | 0.18                 | 1.80        | 0.20             |
| PEO20_15+[NaCl]/[HTAC] = 1/1 | $17.9 \times 10^5$      | 15                      | N/A              | 1.50             | 0.10                 | 1.50        | 0.30             |
| PEO20_15+[NaCl]/[HTAC] = 5/1 | $17.9 \times 10^5$      | 15                      | N/A              | 1.00             | 0.10                 | 1.00        | 0.40             |

$^a c_{PEO}^*$  is the optimum PEO concentration in which maximum drag reduction is obtained.

$^b$ CAC is the critical aggregate concentration: concentration in which surfactant molecules start to interact with polymer

$^c$ CMC is the critical micelle concentration: concentration in which free surfactant micells start to form

$^d$ MBC is the maximum binding concentration: surfactant concentration in which a polymer chain contains a maximum number of surfactant molecules

$^e$ The uncertainties of data determined from surface tension measurement are  $\pm 10\%$

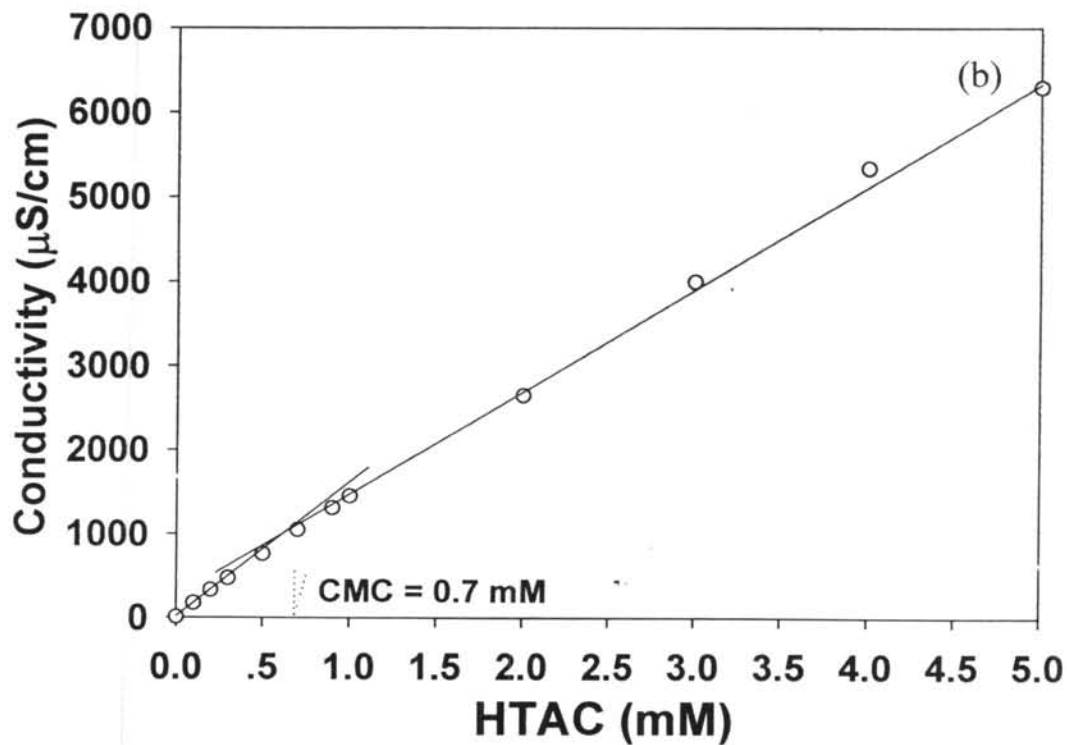
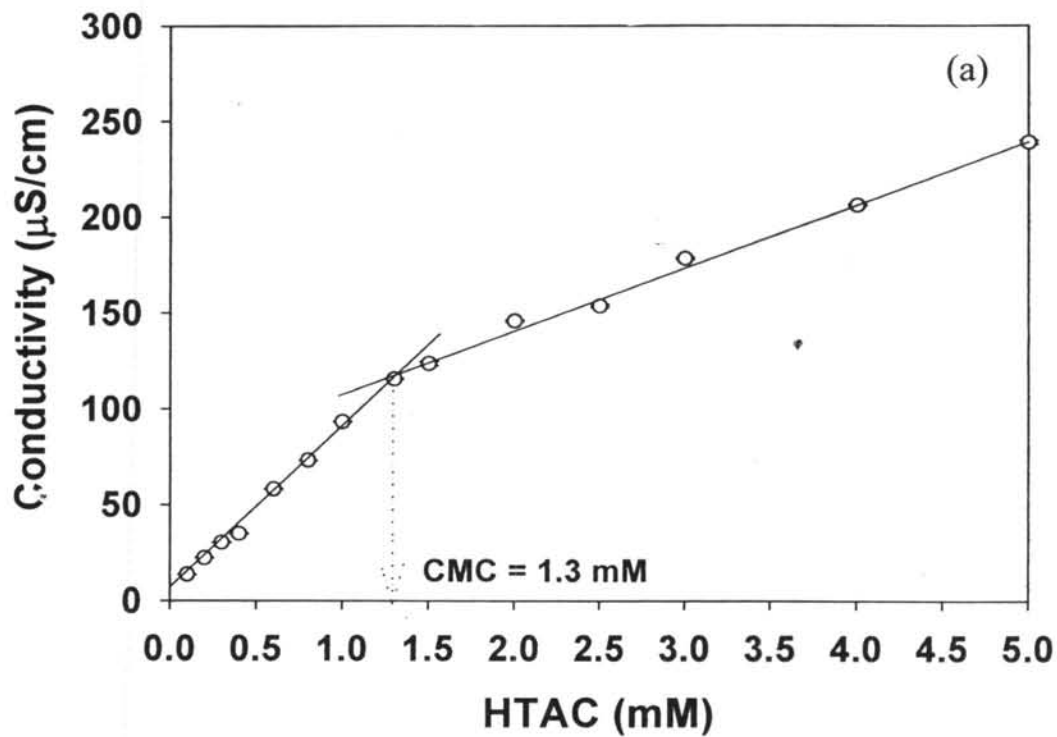
**Table 5.2** Dynamic light scattering data of PEO-HTAC-NaCl complexes quiescent in aqueous solutions at 30°C

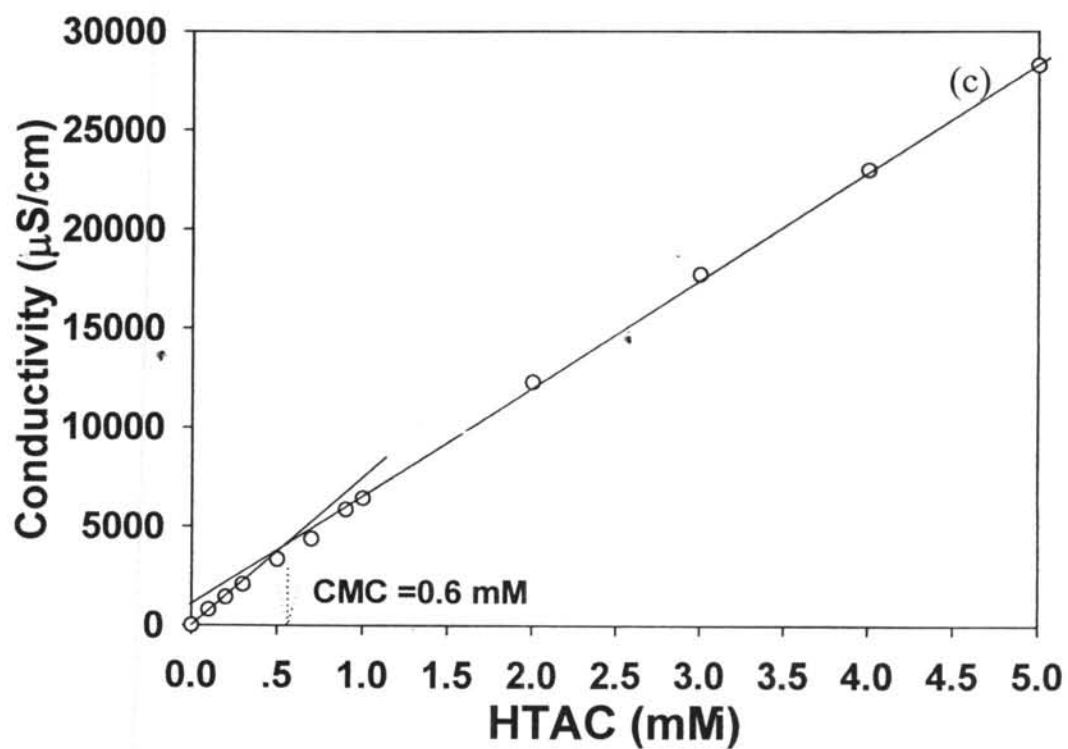
| Codes of system studied                               | $c_{PEO}^*$          |                                      | $D_o \times 10^{12}$<br>(m <sup>2</sup> /s) | $R_h$ (nm) | $\mu_2/\Gamma^2$ |
|---|----------------------|--------------------------------------|---|------------|------------------|
|   | $c_{PEO}^*$<br>(ppm) | (mM of<br>PEO<br>repeating<br>unit ) |   |            |                  |
| <sup>a</sup> HTAC 1.3 mM                              | -                    | -                                    | 170±2.00                                    | 1.31±0.015 | 0.16             |
| <sup>a</sup> HTAC 0.7 mM+[NaCl]/[HTAC] = 1/1          | -                    | -                                    | 99.8±2.04                                   | 2.23±0.045 | 0.17             |
| <sup>a</sup> HTAC 0.6 mM+[NaCl]/[HTAC] = 5/1          | -                    | -                                    | 90.7±1.53                                   | 2.45±0.041 | 0.07             |
| <sup>b</sup> PEO6_40+HTAC 5 mM                        | 40                   | 0.91                                 | 3.98±0.20                                   | 55.9±2.81  | 0.83             |
| <sup>b</sup> PEO6_40+HTAC 5 mM+[NaCl]/[HTAC] = 1/1    | 40                   | 0.91                                 | 4.92±0.03                                   | 45.1±0.23  | 0.21             |
| <sup>b</sup> PEO6_40+HTAC 5 mM+[NaCl]/[HTAC] = 5/1    | 40                   | 0.91                                 | 4.59±0.03                                   | 48.4±0.34  | 0.23             |
| <sup>b</sup> PEO20_15+HTAC 5 mM                       | 15                   | 0.34                                 | 2.40±0.17                                   | 92.7±6.73  | 0.61             |
| <sup>b</sup> PEO20_15+HTAC 5 mM+[NaCl]/[HTAC] = 1/1   | 15                   | 0.34                                 | 3.08±0.05                                   | 72.2±1.21  | 0.25             |
| <sup>b</sup> PEO20_15+HTAC 5 mM+[NaCl]/[HTAC] = 5/1   | 15                   | 0.34                                 | 2.90±0.03                                   | 76.4±0.81  | 0.22             |
| <sup>c</sup> PEO20_15+HTAC 0.2 mM <sup>c</sup>        | 15                   | 0.34                                 | 2.90±0.10                                   | 76.5±0.26  | 0.45             |
| <sup>c</sup> PEO20_15+HTAC 0.2 mM+[NaCl]/[HTAC] = 1/1 | 15                   | 0.34                                 | 3.50±0.06                                   | 63.3±0.11  | 0.35             |
| <sup>c</sup> PEO20_15+HTAC 0.2 mM+[NaCl]/[HTAC] = 5/1 | 15                   | 0.34                                 | 3.22±0.06                                   | 68.9±0.13  | 0.34             |

<sup>a</sup>HTAC concentration is fixed at CMC of each solution

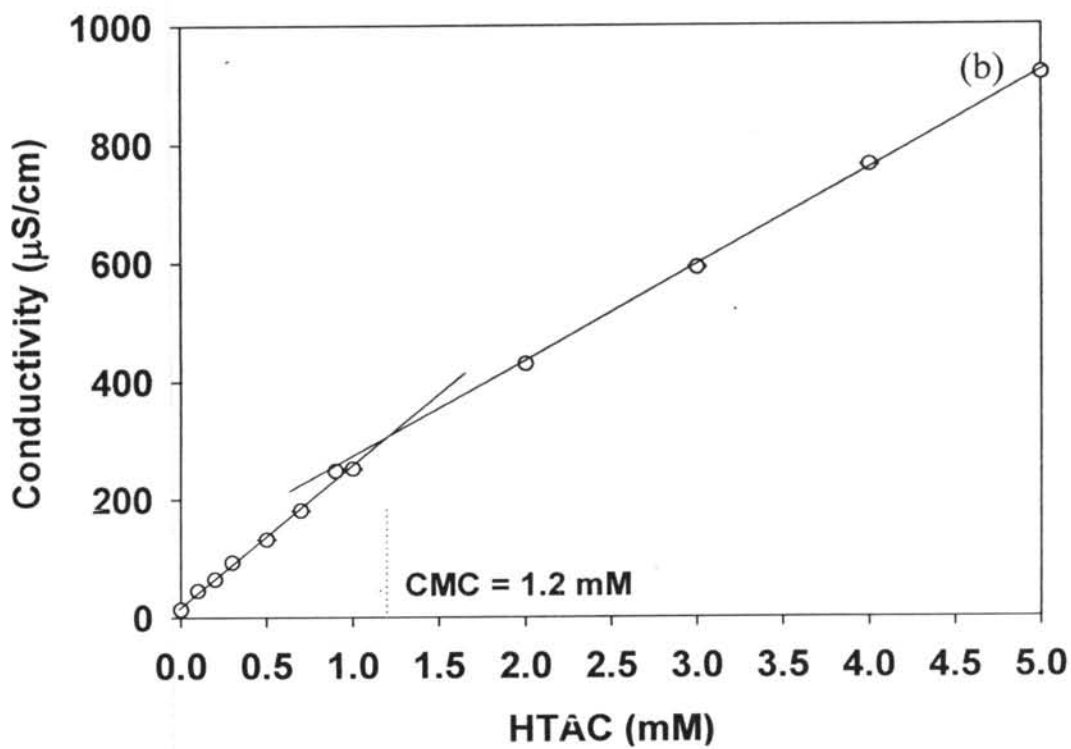
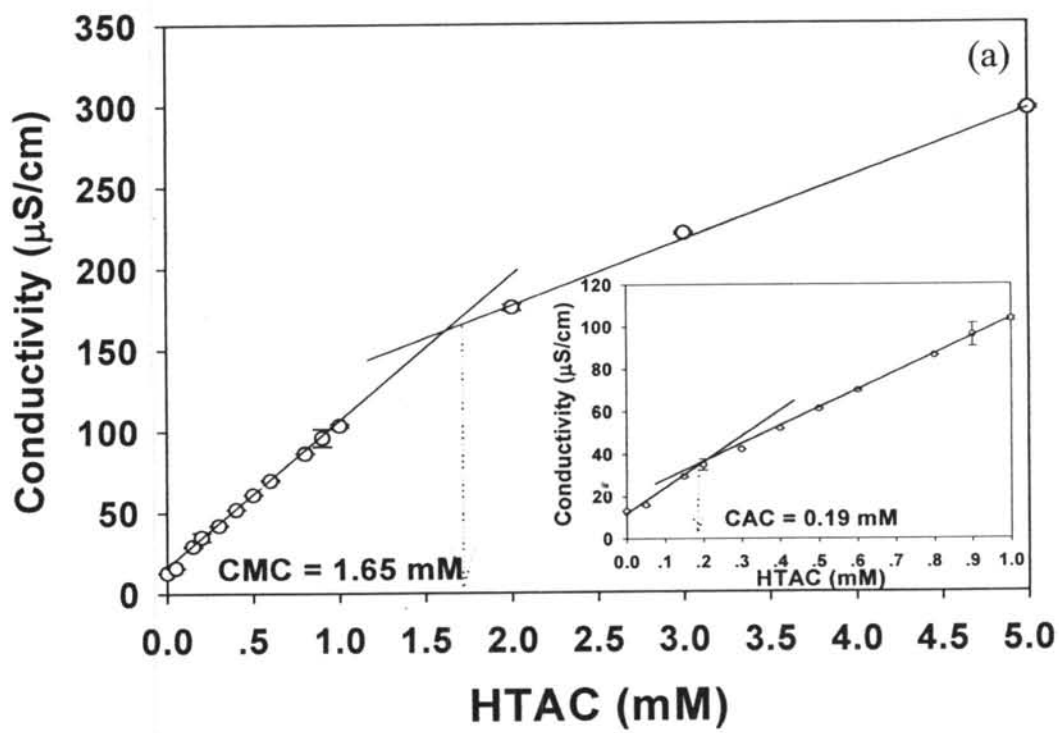
<sup>b</sup>HTAC concentration is fixed at maximum HTAC concentration for wall shear stress measurement

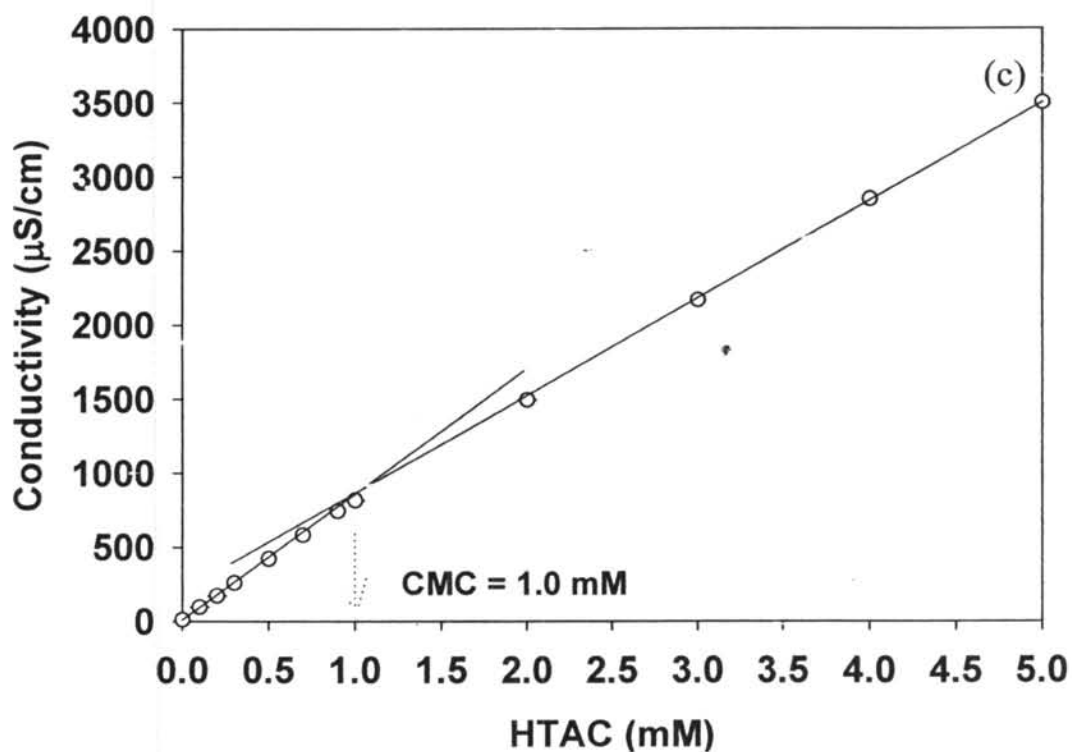
<sup>c</sup>HTAC concentration is fixed at MBC of each solution





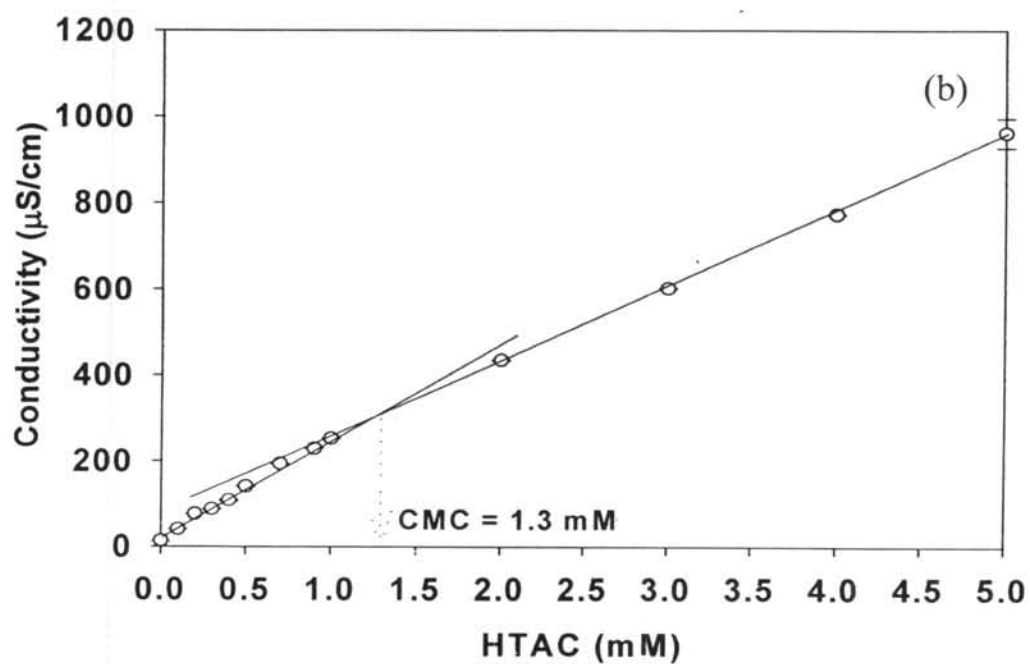
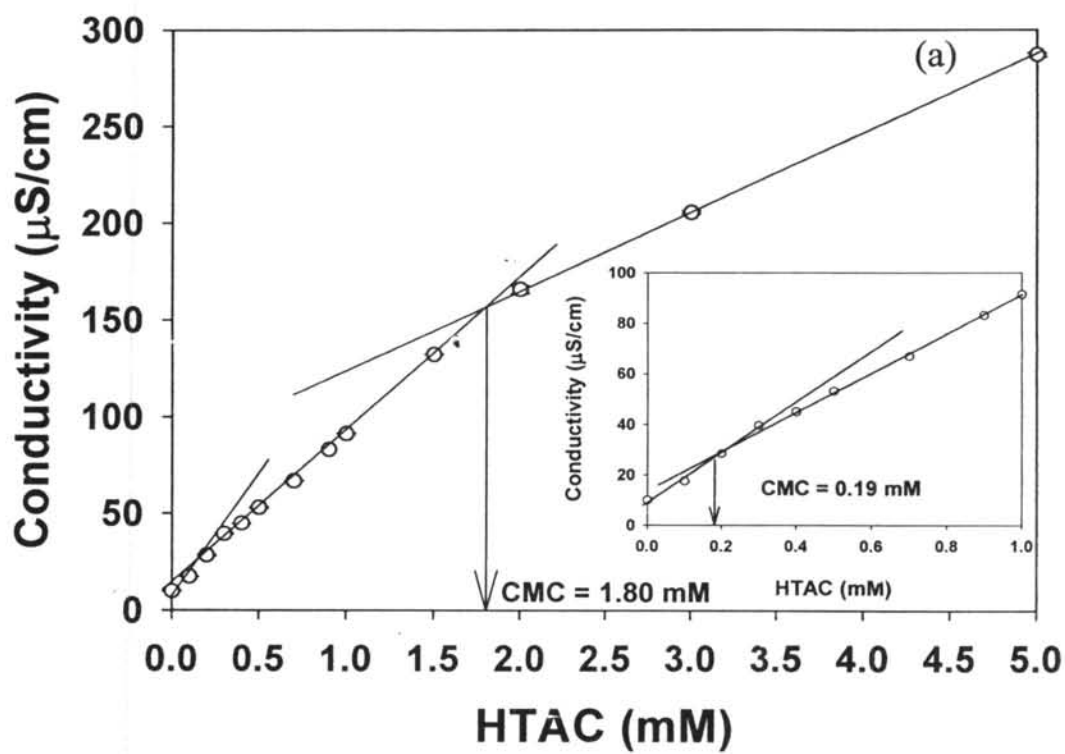
**Figure 5.1** Variation of the conductivity with surfactant concentration at  $30^{\circ}\text{C}$  for aqueous solutions of: (a) pure HTAC; (b)  $[\text{NaCl}]/[\text{HTAC}] = 1/1$ , the mole ratio of NaCl to HTAC equal to one; and (c)  $[\text{NaCl}]/[\text{HTAC}] = 5/1$ , the mole ratio of NaCl to HTAC equal to five.

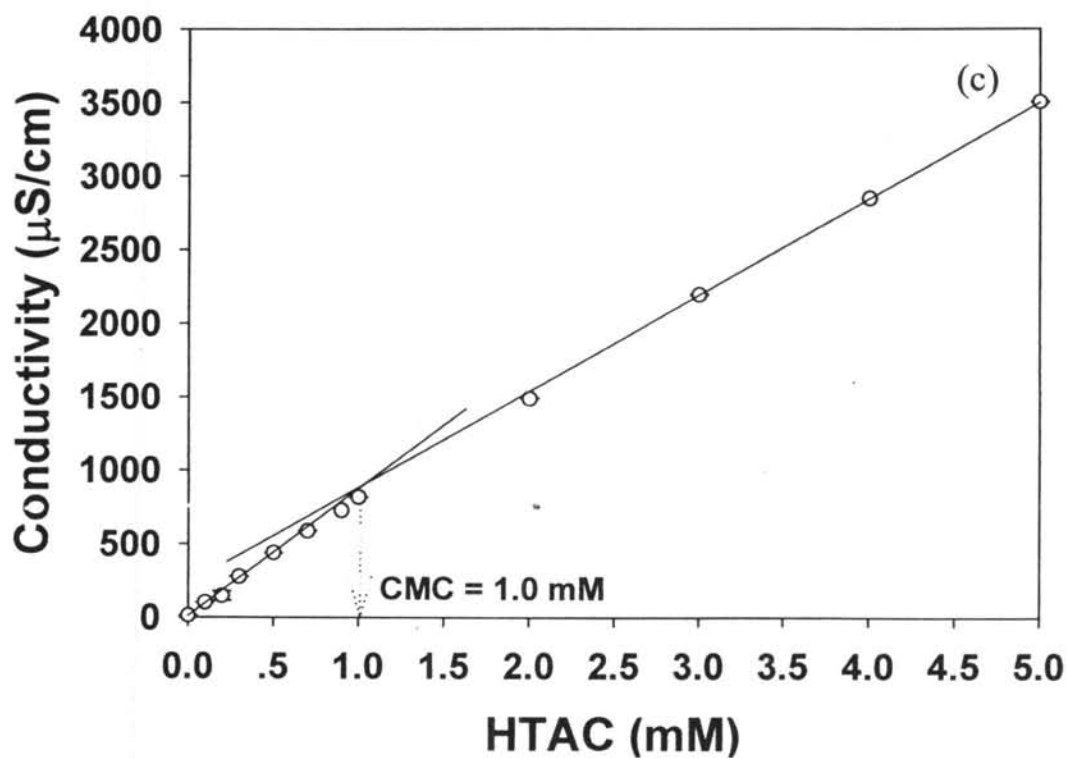




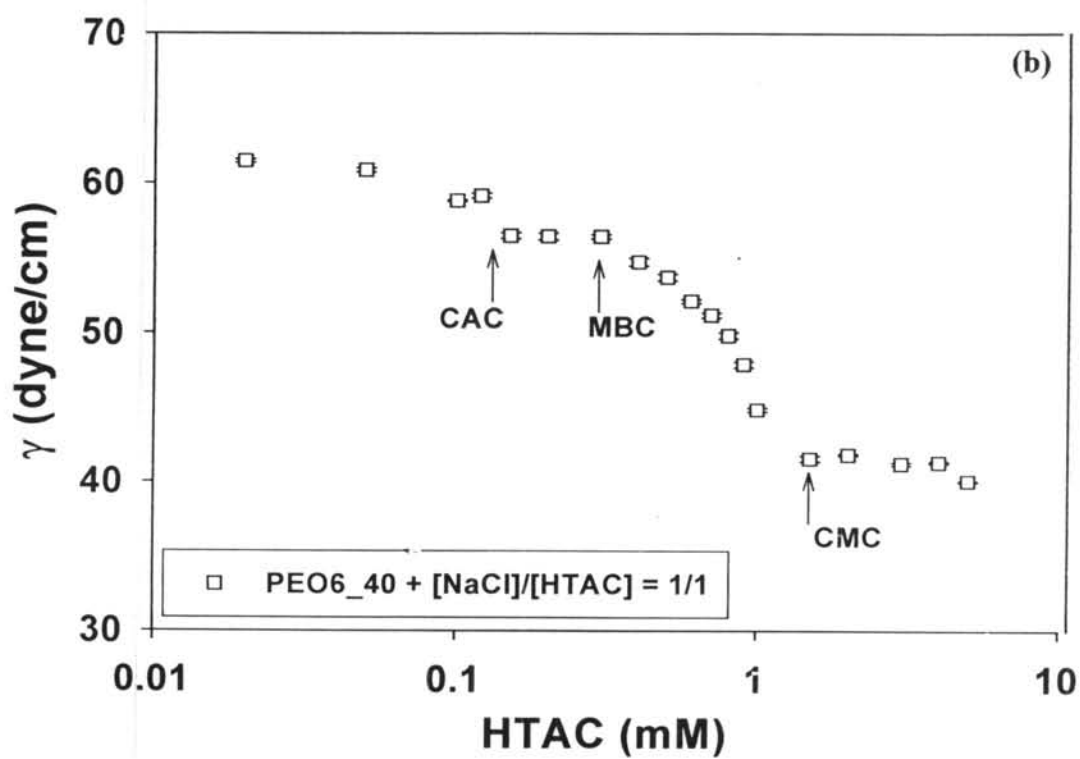
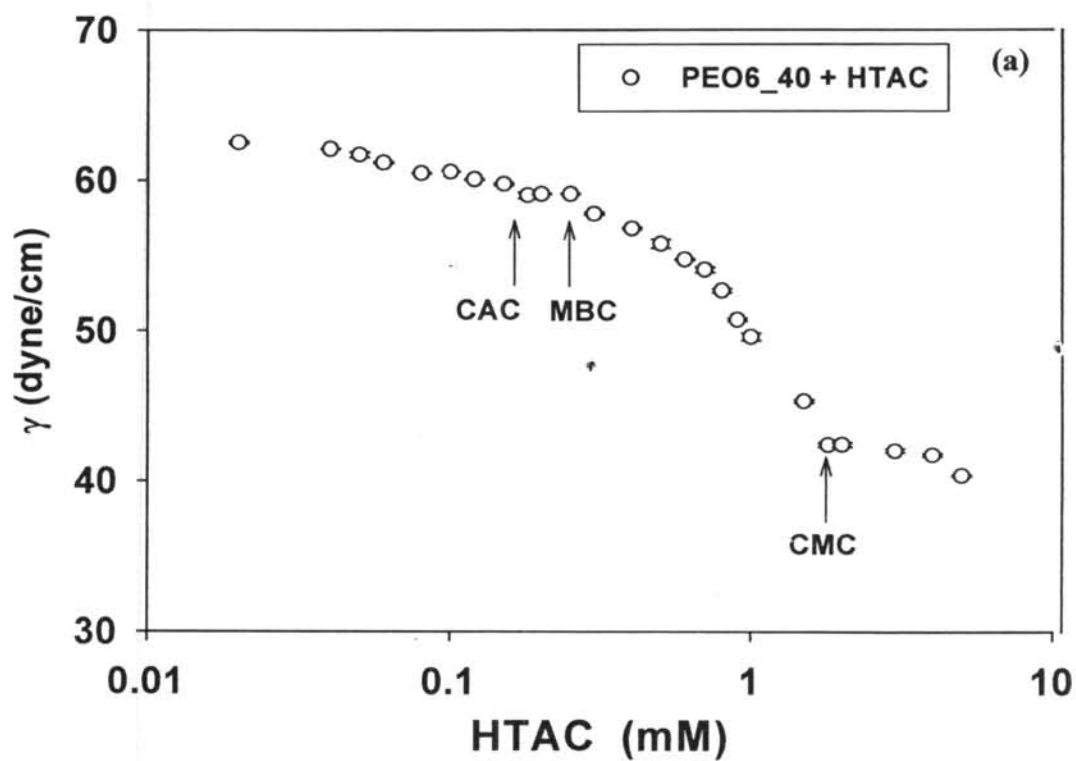
**Figure 5.2** Variation of the conductivity with surfactant concentration at 30°C for aqueous solutions of: **(a)** PEO6\_40 + HTAC, PEO  $M_w$   $6.06 \times 10^5$  g/mol, 40 ppm; **(b)** PEO6\_40 +  $[\text{NaCl}]/[\text{HTAC}] = 1/1$ , PEO  $M_w = 6.06 \times 10^5$  g/mol, 40 ppm, and the mole ratio of NaCl to HTAC equal to one; and **(c)** PEO6\_40 +  $[\text{NaCl}]/[\text{HTAC}] = 5/1$ , PEO  $M_w = 6.06 \times 10^5$  g/mol, 40 ppm, and the mole ratio of NaCl to HTAC equal to five.







**Figure 5.3** Variation of the conductivity with surfactant concentration at 30°C for aqueous solutions of: (a) PEO20\_15 + HTAC, PEO  $M_w = 17.9 \times 10^5$  g/mol 15 ppm; (b) PEO20\_15 +  $[\text{NaCl}]/[\text{HTAC}] = 1/1$ , PEO  $M_w = 17.9 \times 10^5$  g/mol, 15 ppm, and the mole ratio of NaCl to HTAC equal to one; and (c) PEO20\_15 +  $[\text{NaCl}]/[\text{HTAC}] = 5/1$ , PEO  $M_w = 17.9 \times 10^5$  g/mol, 15 ppm, and the mole ratio of NaCl to HTAC equal to five.



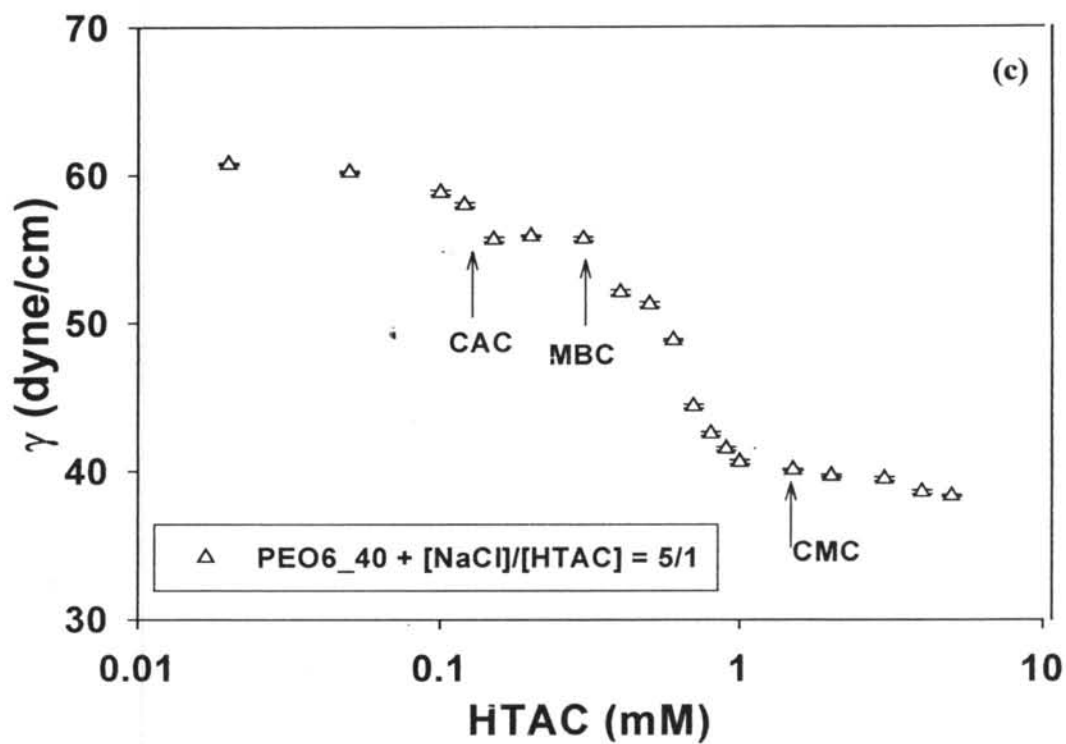


**Figure 5.4** Variation of the surface tension with surfactant concentration at 30°C for aqueous solutions of: (a) PEO6\_40 + HTAC, PEO  $M_w = 6.06 \times 10^5$  g/mol at 40 ppm; (b) PEO6\_40 + [NaCl]/[HTAC] = 1/1, PEO  $M_w = 6.06 \times 10^5$  g/mol, 40 ppm, and the mole ratio of NaCl to HTAC equal to one; and (c) PEO6\_40 + [NaCl]/[HTAC] = 5/1, PEO  $M_w = 6.06 \times 10^5$  g/mol, 40 ppm, and the mole ratio of NaCl to HTAC equal to five.

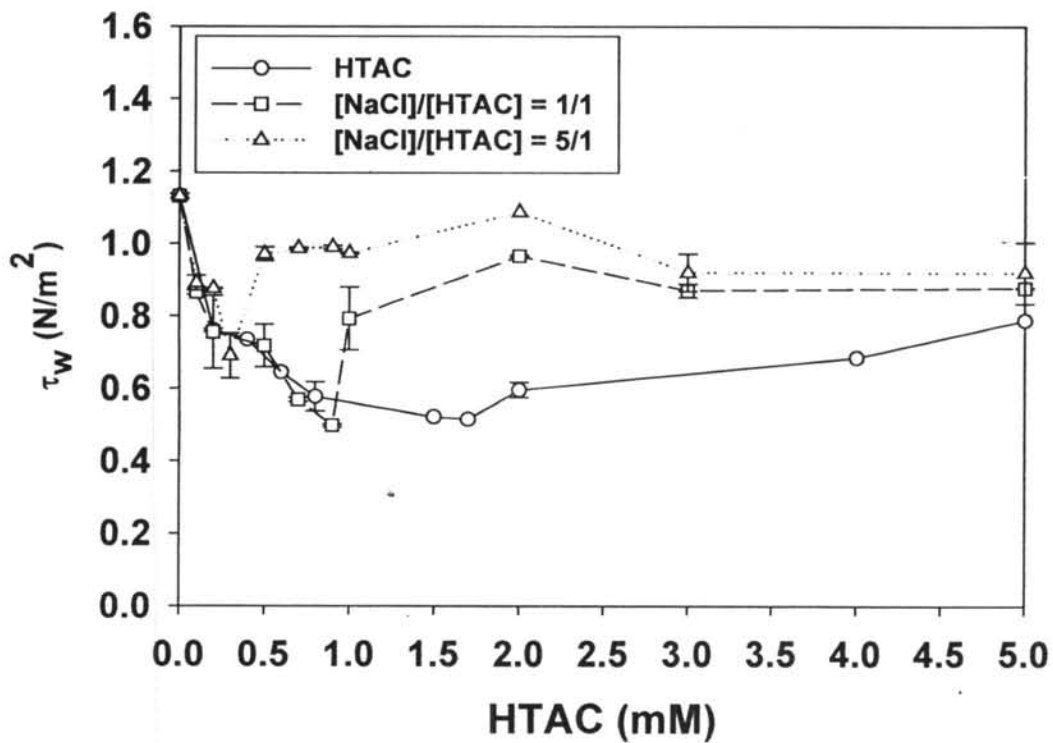


**Figure 5.5** Dependence of wall shear stress,  $\tau_w$ , on HTAC concentration of aqueous HTAC solutions with and without NaCl added at 30 °C,  $Re = 5000$ :

(a) HTAC; (b)  $[NaCl]/[HTAC] = 1/1$ , the mole ratio of NaCl to HTAC equal to one; and (c)  $[NaCl]/[HTAC] = 5/1$ , the mole ratio of NaCl to HTAC equal to five.

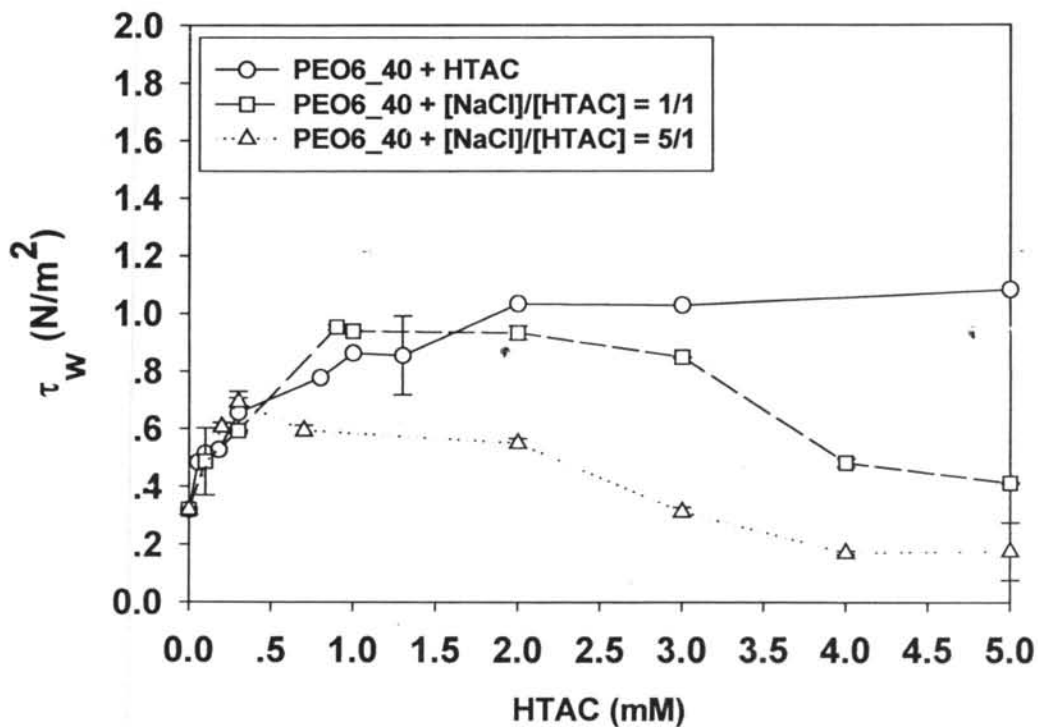


**Figure 5.6** Dependence of wall shear stress,  $\tau_w$ , on HTAC concentration for aqueous PEO6\_40+HTAC solutions with and without NaCl added at 30°C,  $Re = 5000$ :

(a) PEO6\_40 + HTAC, PEO  $M_w$   $6.06 \times 10^5$  g/mol at 40 ppm; (b) PEO6\_40 + [NaCl]/[HTAC] = 1/1, PEO  $M_w$   $6.06 \times 10^5$  g/mol, 40 ppm, and the mole ratio of NaCl to HTAC equal to one; (c) [NaCl]/[HTAC] = 5/1, PEO  $M_w$   $6.06 \times 10^5$  g/mol, 40 ppm, and the mole ratio of NaCl to HTAC equal to five.



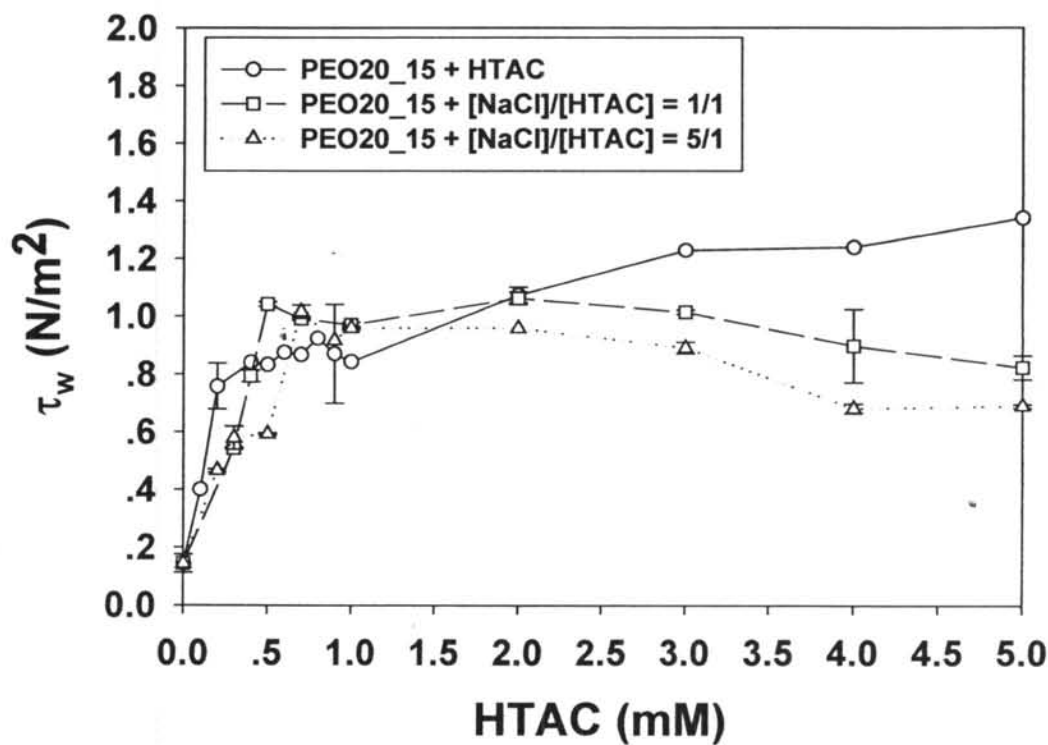


**Figure 5.7** Dependence of wall shear stress,  $\tau_w$ , on HTAC concentration for aqueous PEO20\_15+HTAC solutions with and without NaCl added at 30 °C,  $Re = 5000$ .

(a) PEO20\_15 + HTAC, PEO  $M_w$   $17.9 \times 10^5$  g/mol, 15 ppm; (b) PEO20\_15 + [NaCl]/[HTAC] = 1/1, PEO  $M_w$   $17.9 \times 10^5$  g/mol, 15 ppm, and the mole ratio of NaCl to HTAC equal to one; (c) [NaCl]/[HTAC] = 5/1, PEO  $M_w$   $17.9 \times 10^5$  g/mol, 15 ppm, and the mole ratio of NaCl to HTAC equal to five.

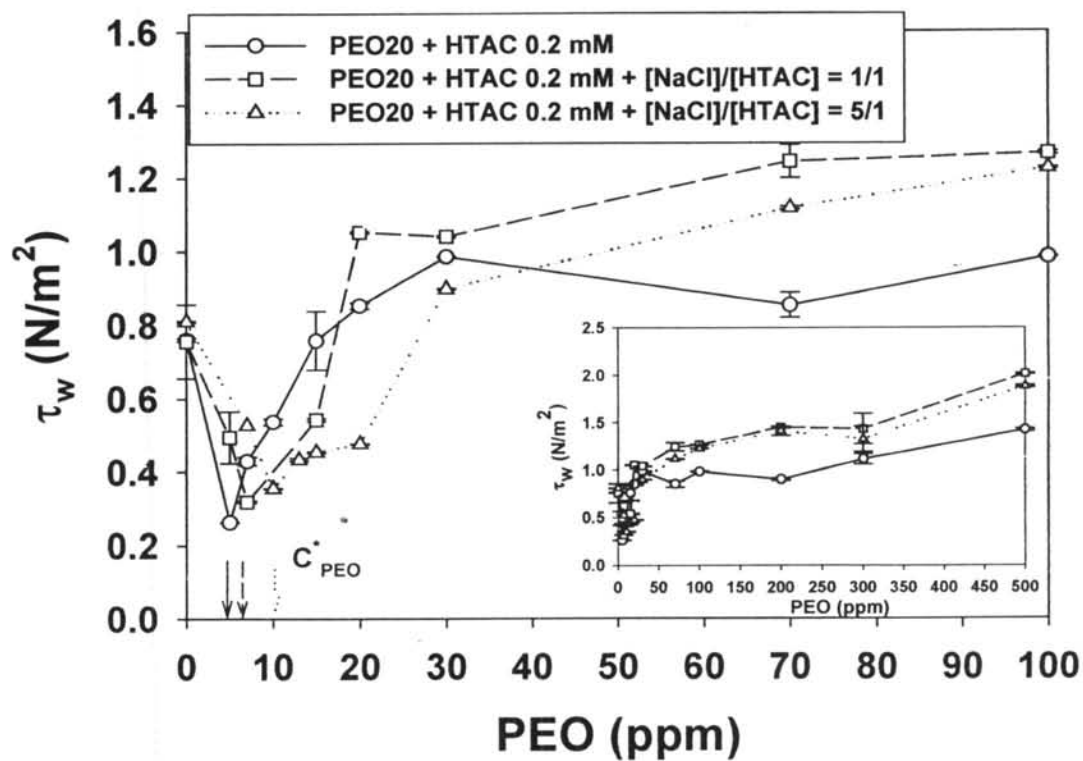


**Figure 5.8** Dependence of wall shear stress,  $\tau_w$ , on HTAC concentration for aqueous PEO20 + HTAC at MBC; PEO  $M_w$   $17.9 \times 10^5$  g/mol and HTAC = 0.2 mM solutions with and without NaCl added at 30 °C,  $Re = 5000$ . (a) PEO20 + HTAC 0.2 mM; (b) PEO20 + HTAC 0.2 mM +  $[NaCl]/[HTAC] = 1/1$ , the mole ratio of NaCl to HTAC equal to one; (c) PEO20 + HTAC 0.2 mM +  $[NaCl]/[HTAC] = 5/1$ , the mole ratio of NaCl to HTAC equal to five.

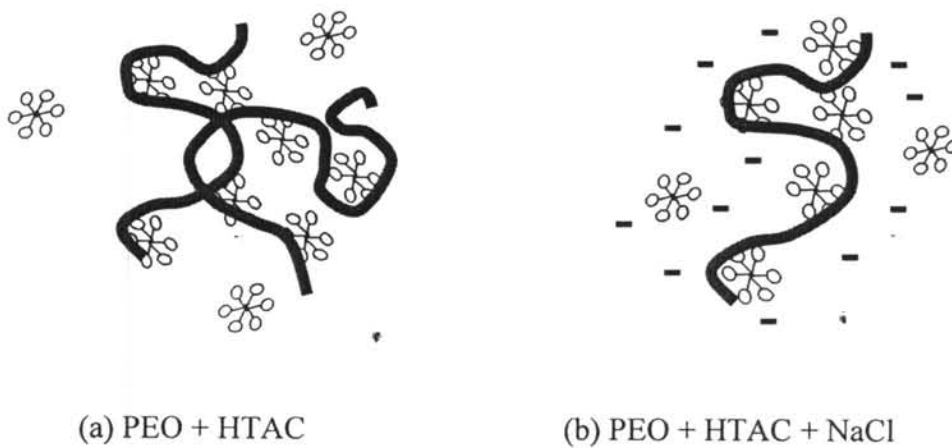


**Figure 5.9** Schematic drawings of complexes formed in PEO + HTAC (a) in the absence and (b) in the presence of NaSal in aqueous solution, respectively, when HTAC concentration is above CMC.